SURFACE PHASE TRANSFORMATION IN LITHIUM ALUMINATE

by

Gordon Mancuso

A senior thesis submitted to the faculty of

Brigham Young University

in partial fulfillment of the requirements for the degree of

Bachelor of Science

Department of Physics and Astronomy

Brigham Young University

August 2008

BRIGHAM YOUNG UNIVERSITY

DEPARTMENT APPROVAL

of a senior thesis submitted by

Gordon Mancuso

This thesis has been reviewed by the research advisor, research coordinator, and department chair and has been found to be satisfactory.

Date	Richard Vanfleet, Advisor
Date	Eric Hintz, Research Coordinator
Date	Ross Spencer, Chair

ABSTRACT

SURFACE PHASE TRANSFORMATION IN LITHIUM ALUMINATE

Gordon Mancuso

Department of Physics and Astronomy

Bachelor of Science

Gamma phase lithium aluminate (γ-LiAlO$_2$) has been proposed as a possible substrate for gallium nitride growth. A corrugation or stripe pattern of beta phase LiAlO$_2$ forms on the surface of γ-LiAlO$_2$ wafers. We attempt to determine the cause of the phase transformation. The beta phase re-forms immediately after removal. This supports the conclusion that the beta phase is more stable at room temperature than the gamma phase, and suggests that the growth of the beta phase is strain limited.

ACKNOWLEDGMENTS

I would like to thank Dr. Vanfleet for his endless insight and answers. I would also like to thank Katie Hurd for teaching me how to use the AFM. Finally, I am in great debt to my wife, Megan, who's patience with me as I completed this work seemed to know no bounds.

This research was supported by the National Science Foundation PHY 0552795 and the BYU Physics Department.

Contents

List of Figures

Chapter 1

Introduction

1.1 Gallium Nitride

Gallium Nitride (GaN) is a wide bandgap semiconductor that is currently used in consumer electronics to create blue light emitting devices and white light LED's. For example, GaN is used in the laser diodes found in Blu-ray recorders and players [1]. It is also used in LED flashlights [2]. GaN is typically grown on a sapphire substrate by metal-organic vapor phase epitaxy (MOVPE) [3]. However, sapphire is not an ideal substrate for the growth of GaN. The lattice mismatch between the two crystals approaches 15%, and the thermal expansion coefficients are different [4]. Both of these lead to large defect densities on the order of $10^{10}/\mathrm{cm}^2$ in the grown GaN [5], which limits its usefulness in many areas. Silicon carbide (SiC) is another substrate that has been used for GaN growth. The SiC lattice more closely matches that of GaN, but its high cost limits its potential [5].

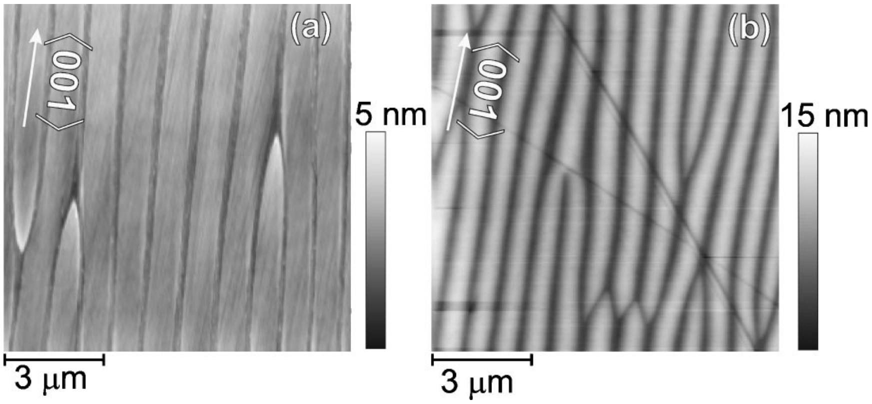

Figure 1.1 Surface corrugation on (a) a typical as-received $LiAlO_2$ wafer and (b) after heating at 750°C. Image from Sun *et al.* [8].

1.2 Lithium Aluminate

Gamma phase lithium aluminate (γ-$LiAlO_2$), which has a tetragonal crystal structure, has been proposed as a possible substrate for GaN growth. $LiAlO_2$ as a substrate has several advantages. It has a small lattice mismatch to GaN (below 1.4% [5]) and is easy to work with [4]. Additionally, GaN grown on $LiAlO_2$ is M-plane, which eliminates a problem known as spontaneous polarization in the GaN. Several groups have grown GaN on $LiAlO_2$, with varying degrees of success [3, 6–9]. Thus far, however, the growth of GaN on $LiAlO_2$ has not been perfected to the point of being commercially viable.

1.3 $LiAlO_2$ Surface Corrugation

A problem that has been identified with $LiAlO_2$ is a corrugation pattern that forms on the surface of the gamma phase wafers [8]. An atomic force microscope (AFM) image of the morphology is shown in Fig. 1.1. The morphology consists of a stripe, mesa, or banding pattern. The morphology on as-received wafers is on the order of a few nanometers high, while HCl etching increases the height to 100 nm or more [10].

The stripes are about a micron wide and can run for hundreds of microns in length along the direction of the γ-$LiAlO_2$'s c axis. The structure of the morphology has been studied by Vanfleet *et al.* [10]. They determined that the mesas themselves are $LiAlO_2$ in the beta phase (see Fig. 1.2), which has an orthorhombic crystal structure, and theorized that the beta phase is more stable than the gamma at room temperature. However, they did not determine the exact cause of formation, nor did they pinpoint when the beta phase begins to form. A schematic of this beta phase formation is shown in Fig. 1.3.

In this work we studied the spontaneous transformation of the gamma phase $LiAlO_2$ to beta phase. Our goal was to determine precisely when in processing the beta phase forms. This will help us to better understand the reason for the phase transformation. Samples of $LiAlO_2$ were subjected to several different processes in an attempt to entirely eliminate the beta phase. The morphology was present after each of these. We concluded that the transformation occurs immediately upon polishing the $LiAlO_2$. This supports the theory that the beta phase is more stable at room temperature than the gamma phase, but is strain limited in its growth.

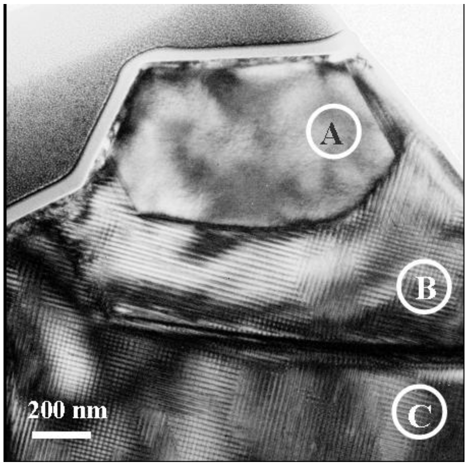

Figure 1.2 TEM bright field image of an etched LiAlO$_2$ wafer in the (001) direction. Labeled regions A, B, and C show: mesas of LiAlO$_2$ in the beta phase, a transitional region displaying lattice strain, and γ-LiAlO$_2$. Image from Vanfleet *et al.* [10].

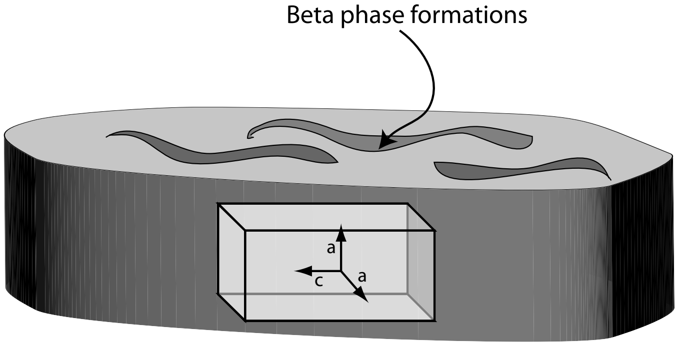

Figure 1.3 Drawing of the basic tetragonal crystal structure. The beta phase is represented running in the c direction on the surface of the wafer.

Chapter 2

Experimental Setup

2.1 Atomic Force Microscopy

An atomic force microscope (AFM) measures surface features. In AFM technology, a small cantilever has a probing tip affixed to the end which travels along the surface of the material being studied. A laser beam focused on the cantilever reflects into a detector. The probe's vertical motion as it travels over surface features translates into deflection of the cantilever. The laser beam reflection responds to this deflection, and the effect is magnified over the length of the beam. The detector tracks the beam response and routes it to a computer program, where the signals are recorded as an image of the surface. Figure 2.1 demonstrates the function of an AFM.

AFM imaging was ideal for our purposes for three reasons. First, we were interested in surface features of lithium aluminate ($LiAlO_2$), and AFM technology is designed for this type of imaging. It images surface features better than other imaging methods, giving a true three-dimensional view of the material. Second, atomic force microscopy is especially sensitive in the direction perpendicular to the sample plane. This allowed detection of surface features that would have been invisible under

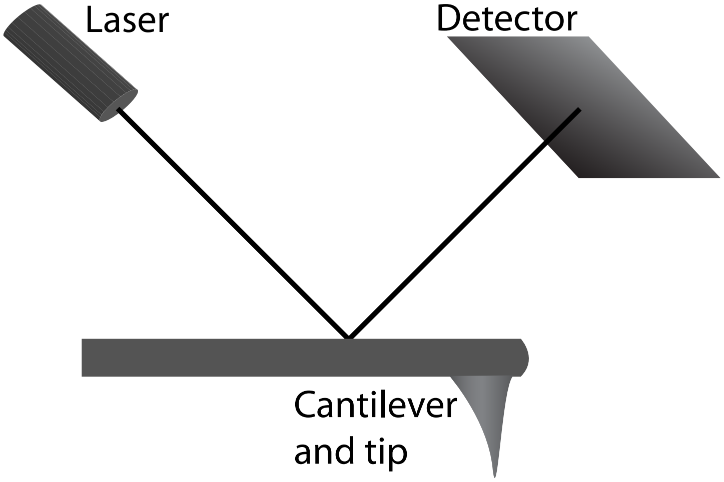

Figure 2.1 Schematic showing the basic function of an AFM.

other microscope technologies. Third, the Dimension 3100 AFM that we used does not require any special sample preparation. This allowed for immediate imaging after polishing.

2.2 LiAlO$_2$ Samples

We had two wafers of LiAlO$_2$ which were originally provided by Crystal Photonics, Inc. One was unaltered in its as-received state; the other had been etched in HCl. The HCl etch enhanced the corrugation by selectively removing the gamma phase material. The wafers are about 200 microns thick and are colorless and transparent. They readily break into smaller pieces, but do not cleave well along any given plane.

We began by ensuring that the surface corrugation would image well under the AFM. We first scanned the LiAlO$_2$ sample that had been etched. Figure 2.2 is

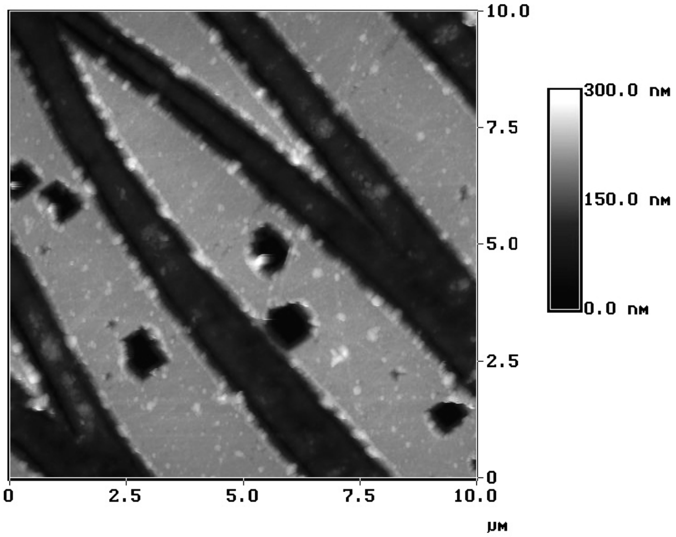

Figure 2.2 AFM micrograph of a sample of $LiAlO_2$. The sample has been etched in HCl.

the micrograph that resulted from this scan. The image clearly displays the beta surface features, showing the morphology to be over 100 nm higher than the adjacent material. A similar image of an unetched sample is shown in Fig. 2.3. Note here that the morphology is clearly visible, but is much smaller in scale.

After we determined that the beta phase features appeared in our samples even after polishing, we acquired a second sample of $LiAlO_2$. We subjected this sample to similar polishing techniques in order to compare with our previous samples. This sample yielded the same beta phase formations as our previous samples.

2.3 Sample Holder

A large portion of this work involved the polishing of $LiAlO_2$. A tripod polisher shown in Fig. 2.4 is suitable for this purpose. An L-bracket is typically affixed to the tripod. Samples are mounted on a glass rod that has been inserted into the

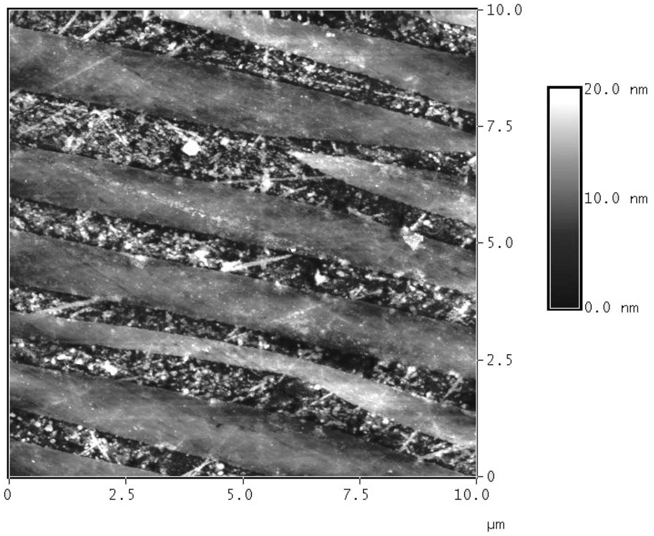

Figure 2.3 AFM image of unetched $LiAlO_2$.

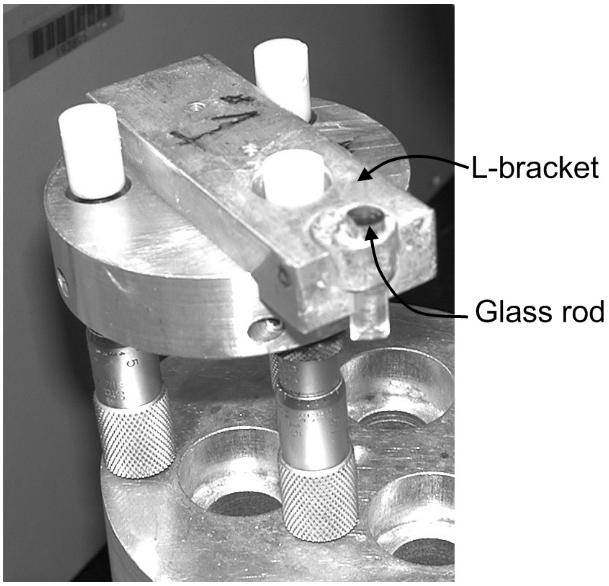

Figure 2.4 Standard tripod polisher. Typically, samples are affixed on the glass rod in the L-bracket, which is attached to the underside of the tripod.

Figure 2.5 Completed aluminum cylinder with glass rod sample holder cemented in place.

bracket. This polishing setup works well for transmission electron microscopy (TEM) sample preparation as it yields wedge shaped samples. However, since we were more interested in surface features, we did not want to polish at an angle—rather, polishing flat on the samples was desired. To accomplish this, we machined a small cylinder piece that could be affixed to the tripod polisher (see Fig. 2.5). The glass rod length is about 1.2 cm, as that is the maximum height which can fit underneath the AFM head. By keeping the rod below this length, a freshly polished sample could be imaged immediately on the AFM. The rod was affixed in the center hole with epoxy, and two holes were threaded for attachment of the piece to the tripod.

2.4 Polishing Method

The surface mesas can be over 100 nm high, as shown in Fig. 1.2. We could ensure the complete removal of existing beta phase material on the surface by polishing off several microns of $LiAlO_2$. If any beta phase was then visible under micrograph, we would know it was newly formed. We began the polishing process by cleaving a piece of $LiAlO_2$ from one of the received samples. This piece was small enough to fit on the tip of the 0.5 cm diameter glass rod, where it was mounted using mounting wax. It was useful to make a small sketch of the sample, which helped in determining which side had been polished once the sample was removed from the rod.

Once the sample was affixed to the tripod, it was polished with a 30 μm aluminum oxide (Al_2O_3) lapping film. Lapping films are basically high precision pieces of sandpaper. The film was placed on a polishing wheel, which can rotate at up to 500 rpm. We began the process with a large grit size to ensure that all of the beta phase morphology was removed during polishing. Once enough material was removed to ensure removal of the surface morphology, the sample was polished with progressively smaller grit sizes, using both Al_2O_3 and diamond lapping films. The final polish was a 0.05 μm diamond suspension. Attempts to use colloidal silica as a final polish met with interesting results (see Sec. 3.2).

2.5 Attempts at Morphology Removal

To understand the beta phase growth, we tried a variety of processes in an attempt to inhibit or enhance its formation. Table 2.1 lists these along with the result of each. The results of these are covered in greater detail in Chap. 3.

Process	Result
Vary polishing direction	Beta remains
Acid etch	Beta remains
Polish with colloidal silica	Brings out the beta phase
Omit various steps	Led to dirtier samples, but beta remains
Oil based suspension polish	Beta remains
Use methanol as polishing coolant	Beta remains
Heat to 1000°C for one hour	Beta remains
Polish on both sides of sample	Beta remains
Polish on second a face	Beta remains

Table 2.1 A list of attempts to remove the beta phase.

Chapter 3

Results and Conclusion

3.1 Beta Phase Re-forms

We polished several samples using our standard polishing procedure (see Sec. 2.4), then imaged them immediately following polishing (see Figs. 3.1 and 3.2). In both of these, special care was taken to polish as well as possible so that the beta phase would not be obscured by polishing marks. In Fig. 3.1, we see polishing marks running from the bottom left to the top right. We deliberately polished in a direction somewhat perpendicular to the morphology direction to see if that had any effect on the phase transformation. At first glance, the surfaces appear to be fairly flat, with minimal features even with a vertical scale of 10 nm over a 10 μm surface. Note, however, that closer inspection shows evidence of beta phase mesas in the horizontal direction. The pattern is even more pronounced in Fig. 3.2. Here the small polishing marks can be seen almost exactly perpendicular to the beta phase features. The presence of the features immediately after polishing supports the conclusion that the beta phase is more stable at room temperature.

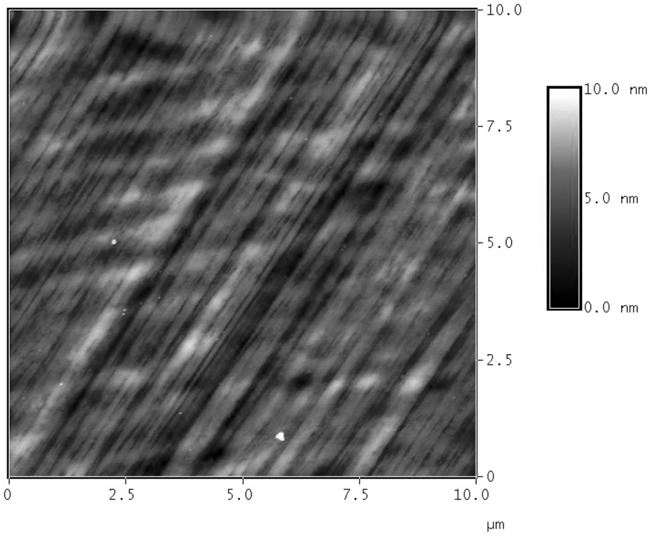

Figure 3.1 Diamond polished $LiAlO_2$. Beta phase morphology seen on a just-polished wafer. The formations run horizontally across the image, while polishing marks run from the bottom left to upper right.

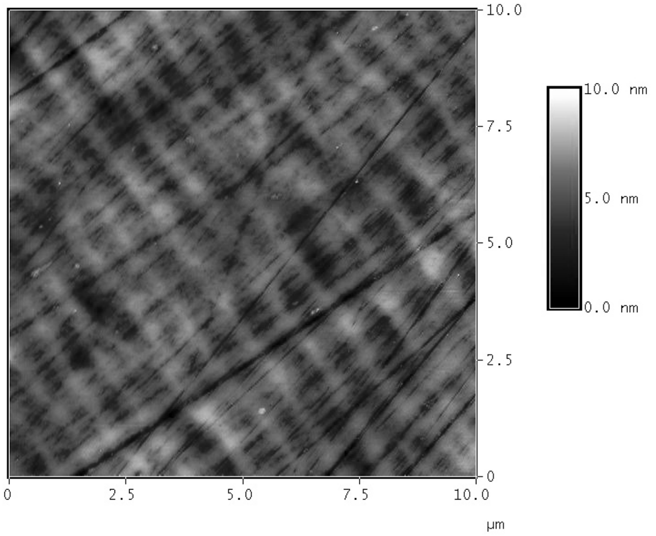

Figure 3.2 Diamond polished $LiAlO_2$. More pronounced beta phase mesas seen immediately after polishing. The mesas run from the upper left to the bottom right, with polishing marks almost exactly perpendicular.

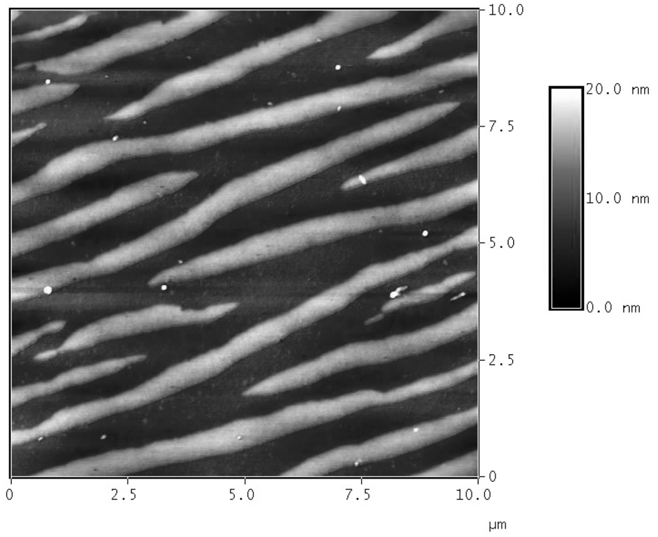

Figure 3.3 $LiAlO_2$ polished with colloidal silica. The morphology is clearly seen. Note that polishing marks are almost nonexistent.

3.2 Colloidal Silica

Colloidal silica is a colloid of silica (SiO_2) particles used for polishing. It typically yields very smooth surfaces. Diamond suspensions use physical abrasion for polishing, so scratches are easily seen on the surface under AFM, even when the sample has been polished with 0.05 μm diamond suspension. However, colloidal silica gives a better finish with its similarly sized particles. This is because colloidal silica also performs a kind of chemical polish. We attempted to use colloidal silica as a final polish for $LiAlO_2$. Figure 3.3 shows the result of such a polish. While the surface was left virtually scratch-free, the colloidal silica brought out the beta phase features. We see that the features are several times higher than those seen after a simple diamond polish.

3.3 Other Attempts

To strengthen the theory that the beta phase is more stable at room temperature than the gamma phase, we attempted several different processes to ensure that no part of the sample preparation process was causing the mesa formation. These are listed in Table 2.1. Some of these have already been discussed. We will now explain the others, devoting more space to those that are particularly interesting.

After polishing a sample, it was typically cleaned before AFM imaging. We omitted each step of the cleaning process to make sure that no particular chemical was responsible for the beta phase formation. The beta phase still formed after each of these omissions. We also tried using different polishing techniques. Specifically, we polished with an oil based diamond suspension and also tried polishing with methanol instead of water as a coolant. Both of these similarly yielded beta phase formations.

We also acid etched samples in several acids: hydrochloric, sulfuric, phosphoric, nitric, and acetic. With the exception of acetic acid, which did not etch the $LiAlO_2$ at all, all of these acids selectively etched the gamma phase material over the beta phase material. This left the beta phase mesas standing much higher than the surrounding material.

3.3.1 Heating

Vanfleet *et al.* have shown that at about 450°C, the beta phase converts back to gamma phase [10]. We had an idea that perhaps threads of beta phase were located throughout the sample and were simply being exposed by the polishing. To check if this could be the case, we heated a sample to 1000°C for one hour to make sure any beta phase was converted to gamma. We polished and imaged the sample. Figure 3.4 shows that the beta phase still appeared.

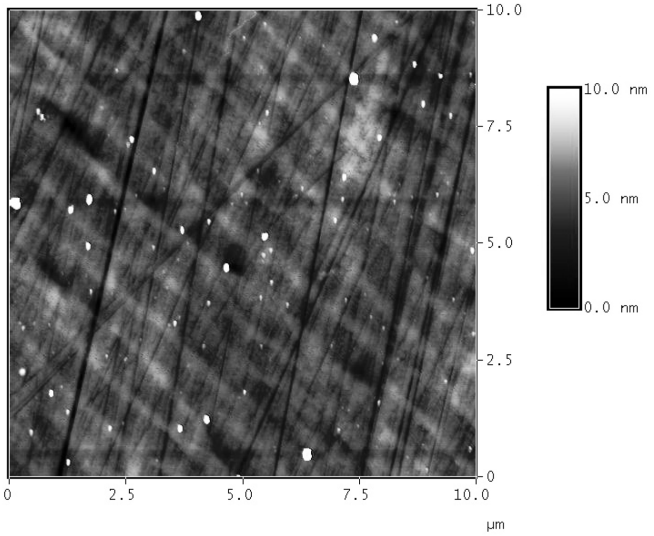

Figure 3.4 Side 1 of a $LiAlO_2$ sample that has been heated to 1000°C for one hour, then diamond polished.

3.3.2 Flipping the Sample

Sun *et al.* have shown that the two sides of a $LiAlO_2$ wafer behave somewhat differently [8]. They showed that the morphology is about five times more pronounced on one side versus the other. We polished both sides of a $LiAlO_2$ sample to find any differences. Figures 3.4 and 3.5 show that the beta phase forms just as readily on either side.

3.3.3 Side View

Gamma phase $LiAlO_2$ has a tetragonal crystal structure. As Fig. 3.6 shows, there are two perpendicular a crystal directions. Since all of our samples were from the same wafers, all of our polishing was on the same a surface. There was the possibility that polishing on the other a surface would affect the formation of the beta phase. To polish on the other a direction requires polishing on the side of a wafer. This is

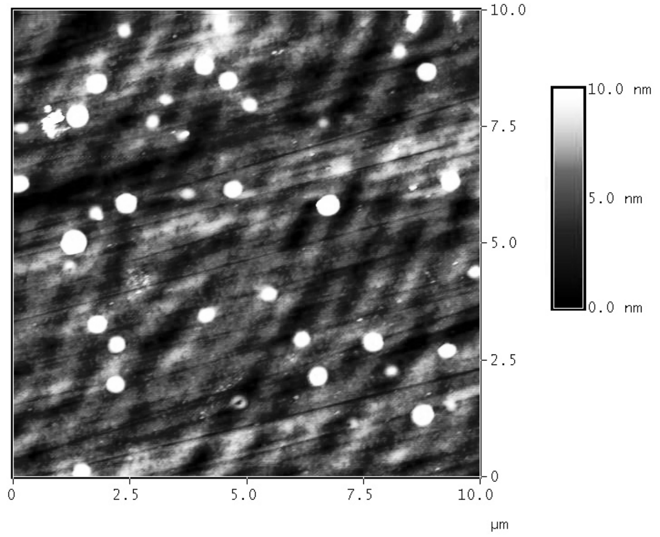

Figure 3.5 Side 2 of a $LiAlO_2$ sample that has been diamond polished. Note that the beta phase is still visible.

not done easily. We found the direction of the beta phase growth on a sample, then mounted the sample between two pieces of glass as in Fig. 3.7. This added strength allowed the sample to be mounted on the sample holder on its side. The sample was polished and imaged. As can be seen in Figs. 3.8 and 3.9, the beta phase is still visible, though it does appear distorted. We attribute this to the fact that the piece was probably not mounted at precisely the right angle to polish flat on the second *a* face.

3.4 Formation Theory

Every process performed on the $LiAlO_2$ points to the conclusion that the beta phase re-forms immediately upon surface polishing. This supports the theory that the beta phase is more stable at room temperature. The fact that the beta phase structures form in bands along the *c* axis of the gamma phase material also supports the idea

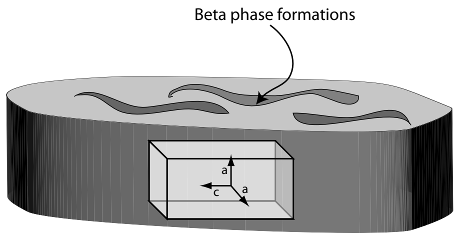

Figure 3.6 Drawing of the basic tetragonal crystal structure. The beta phase is represented running in the c direction on the surface of the wafer.

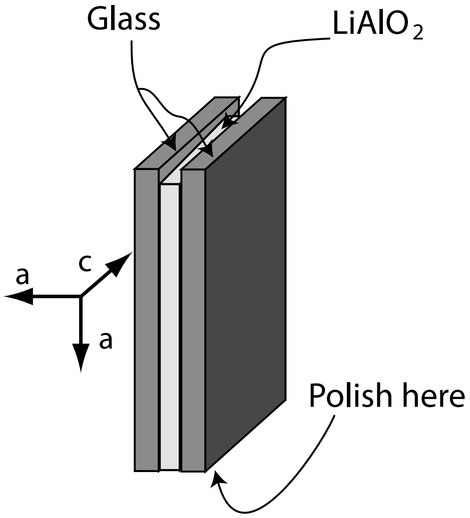

Figure 3.7 A piece of $LiAlO_2$ was mounted between two pieces of glass.

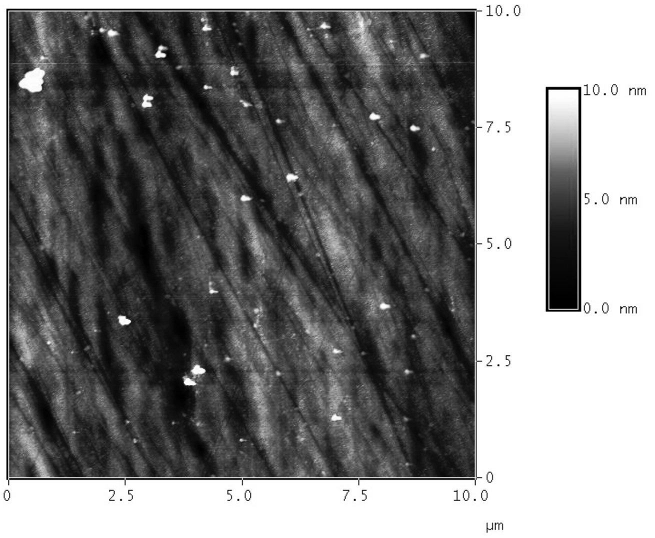

Figure 3.8 Second *a* face of a $LiAlO_2$ wafer that has been diamond polished.

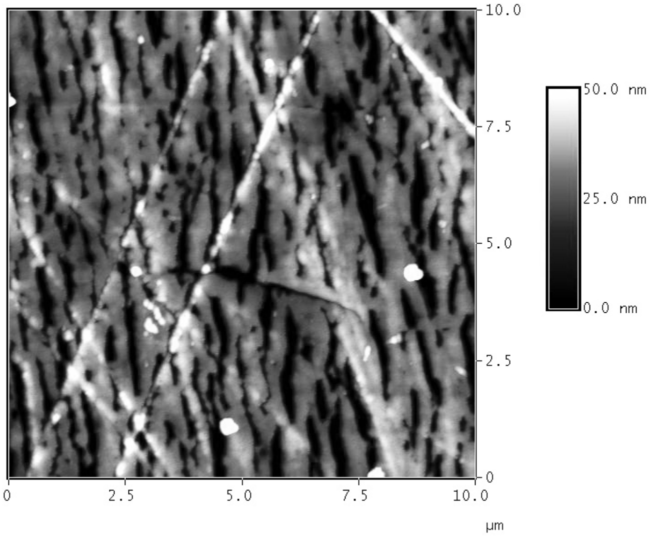

Figure 3.9 Second *a* face of a $LiAlO_2$ wafer that has been polished with colloidal silica.

of strain limiting the growth of the beta phase.

Figure 3.10 gives a basic outline of the theory of beta phase growth. We start with the premise that the beta phase is more stable than the gamma phase. The relative freedom at the surface of a γ-LiAlO$_2$ sample allows the gamma phase lattice to realign to the thermodynamically more stable beta phase. As this transformation proceeds, strain due to lattice mismatch builds up at the boundary between the beta phase and the gamma phase. At some point, the strain becomes large enough to make the transformation thermodynamically unfavorable. Along the c axis, however, the strain is minimal, allowing long mesas to form in that direction. We can understand this quantitatively by examining the crystal structures of the beta and gamma phases.

γ-LiAlO$_2$ has a tetragonal lattice structure (space group P4$_1$2$_1$2) with lattice constants of $a = 0.5168$ nm and $c = 0.6268$ nm [11]. The beta phase is orthorhombic (Pna2$_1$) with lattice constants $a = 0.528$ nm, $b = 0.630$ nm, and $c = 0.490$ nm. Experimentally, the beta b axis aligns with the gamma c axis (0.630 nm with 0.6268 nm, 0.5% mismatch), the beta a axis aligns with the in-plane gamma a axis (0.528 nm with 0.5168 nm, 2.2% mismatch), and the beta c axis aligns with the out-of-plane gamma a axis (0.490 nm with 0.5168 nm, 5.2% mismatch). There is also a very good match in the lowest mismatch directions with the actual atomic positions [10]. The largest mismatch is in the out of plane direction where growth of the beta phase would cause significant stress. Growth of the beta phase in the in-plane a direction would cause less (but still significant) stress, while growth in the in-plane c direction would cause very little stress. Thus, long mesas form along the c direction while the increase in stress limits the growth in the other two directions.

Diamond polishing easily removes the beta phase as well as the gamma phase material. This is why we see such small and faint formations on samples that have been diamond polished. The beta phase forms after polishing has finished, and the

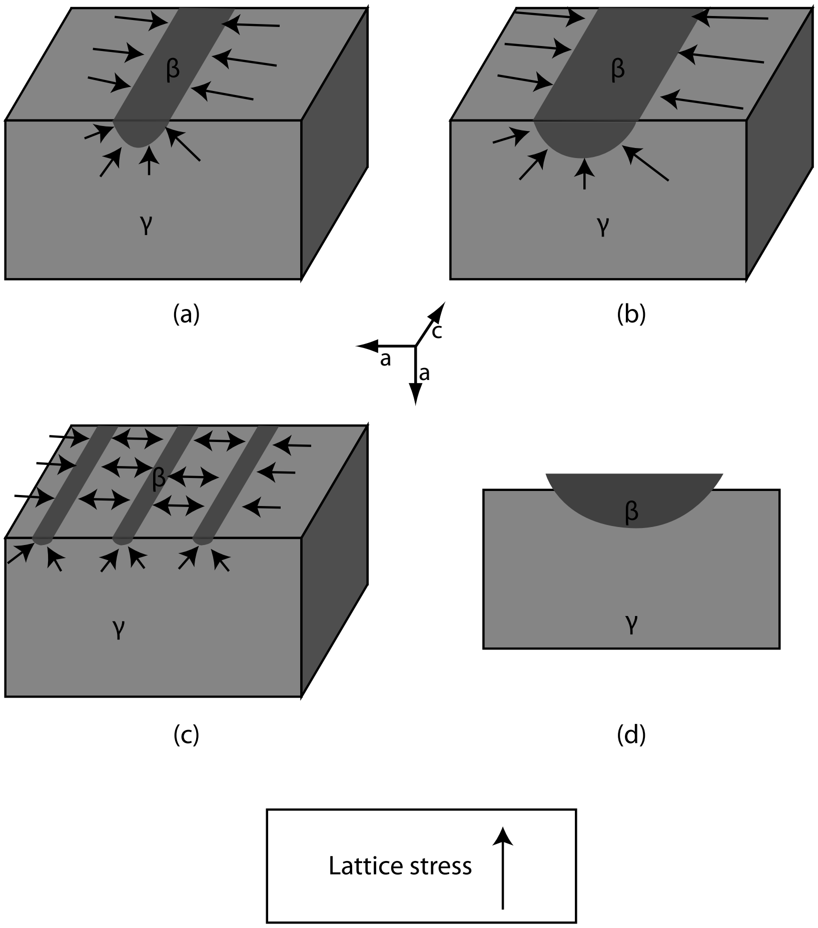

Figure 3.10 A schematic diagram outlining the theory of the beta phase formation. (a) The beta phase begins to form on the surface. It propagates in the *c* direction but is strain limited in the *a* directions. (b) At some point the strain buildup prevents any further phase transformation. (c) A diamond polished wafer exhibits smaller beta features as the diamond easily removes the beta phase. The beta phase forms only after polishing is finished. (d) Colloidal silica polishing removes the gamma phase but not the beta phase. This relieves stress, allowing the beta phase features to grow.

formation size is quickly limited by lattice strain. However, colloidal silica polishing yields much larger and well-pronounced beta phase formations. We believe there are two reasons for this. First, it appears that colloidal silica selects the gamma phase over the beta. This by itself would increase the relative size of the beta phase formations as the surrounding gamma phase material is removed. As the gamma phase is cleared away, the lattice strain would also decrease, allowing the beta phase to grow in size. Second, since colloidal silica does not remove the beta phase as diamond does, the beta phase has a chance to grow during the polishing process. This "massaging" of the crystal lattice allows the structure to seek more stable arrangements, yielding still more pronounced beta phase structures.

3.5 Conclusion

The most important finding of this work is that beta phase formations appear on the surface of γ-$LiAlO_2$ samples immediately after polishing. This supports the hypothesis that the beta phase is more stable than the gamma phase at room temperature. We were able to give this theory more support as we observed the phase transformation no matter what was done to the $LiAlO_2$. We also give evidence that the beta phase growth is strain limited in the a directions, but not in the c direction.

Bibliography

[1] "Sony Global - Laser Diode," http://www.sony.net/Products/SC-HP/laserdiodewld/tec/index03.html (Accessed 9 July 2008).

[2] "LED Flashlight Colors and Applications Guide and Color Characteristics," http://www.led-flashlight-store.com/colors-applications-guide.html (Accessed 9 July 2008).

[3] H. P. Maruska, D. W. Hill, M. C. Chou, J. J. Gallagher, and B. H. Chai, "Free-standing non-polar gallium nitride substrates," Opto-Electron. Rev. **11,** 7 (2003).

[4] M. M. C. Chou, S. J. Huang, and C. W. C. Hsu, "Crystal growth and polishing method of lithium aluminum oxide crystal," J. Crystal Growth **303,** 585 (2007).

[5] M. M. C. Chou, H. C. Huang, D.-S. Gan, and C. W. C. Hsu, "Defect characterizations of γ-$LiAlO_2$ single crystals," J. Crystal Growth **291,** 485 (2006).

[6] R. R. Vanfleet, J. A. Simmons, H. P. Maruska, D. W. Hill, M. M. C. Chou, and B. H. Chai, "Defects in m-face GaN films grown by halide vapor phase epitaxy on $LiAlO_2$," Appl. Phys. Lett. **83,** 1139 (2003).

[7] P. Waltereit, O. Brandt, M. Ramsteiner, R. Uecker, P. Reiche, and K. H. Ploog,

"Growth of M-plane GaN($1\bar{1}00$) on γ-LiAlO_2(100)," J. Crystal Growth **218,** 143 (2000).

[8] Y. J. Sun, O. Brandt, and K. H. Ploog, "Growth of M-plane GaN films on γ-LiAlO_2," J. Vac. Sci. Technol. B **21,** 1350 (2003).

[9] M. M. C. Chou, D. R. Hang, H. Kalisch, R. H. Jansen, Y. Dikme, M. Heuken, and G. P. Yablonskii, "Crystal growth and properties of LiAlO_2 and nonpolar GaN on LiAlO_2 substrate," J. Appl. Phys. **101,** 103106 (2007).

[10] R. R. Vanfleet, J. A. Simmons, D. W. Hill, M. M. C. Chou, and B. H. Chai, "Anti-Phase Ordering and Surface Phases in Lithium Aluminate," (Submitted to J. Appl. Phys.).

[11] M. Marezio, "The Crystal Structure and Anomalous Dispersion of γ-LiAlO_2," Acta Cryst. **19,** 396 (1965).